Power and Particle Exhaust Control in All W ASDEX Upgrade

R. Neu[1], J.C. Fuchs[1], A. Kallenbach[1], R. Dux[1], T. Eich[1], R. Fischer[1], O. Gruber[1], A. Herrmann[1], A. Janzer[1], H.W. Müller[1], T. Pütterich[1], J. Rapp[2], V. Rohde[1], K. Schmid[1], J . Schweinzer[1], M. Sertoli[1], G. van Rooij[2] and the ASDEX Upgrade Team[1]

[1]Max-Planck-Institut für Plasmaphysik, EURATOM Association, D-85748 Garching, Germany
[2]FOM-Institute for Plasma Physics Rijnhuizen, Association Euratom-FOM, Trilateral Euregio Cluster, 3430 BE, Nieuwegein, The Netherlands

E-mail contact of main author: Rudolf.Neu@ipp.mpg.de

Abstract Independent of the plasma facing materials in future fusion devices impurity seeding will become an inevitable element of the operation to protect the divertor from excessive heat loads. A very beneficial behaviour in terms of reduced power loads, moderate impurity concentrations and increased confinement has been found in N_2 seeded discharges in ASDEX Upgrade. Radiative cooling has been applied in a large variety of plasmas ranging from improved H-Modes at intermediate density and heating power to discharges with very high heating power ($P_{aux} \approx 20$ MW) or high density and radiation fraction exploring the type-III ELM regime. Generally, the radiated power from the X-point and divertor region increased in N_2 seeded discharges by more than a factor of two, but the core radiation is almost unchanged. Similarly, also the radiation during type-I ELMs is increased. In unseeded discharges with a pure tungsten wall, about 20% of the ELM energy is radiated, which is clearly less than in earlier discharges with mixed carbon and tungsten PFCs. For nitrogen seeded discharges, however, the ELM energy is generally smaller, and up to 40% of the ELM energy is radiated. This value is comparable to that found in former campaigns with mixed C/W PFCs. Consequently,the power load to the divertor targets during and in between type-I ELMs drops significantly with nitrogen seeding. Even for discharges at highest heating power, good energy confinement could be obtained simultaneously with a low impurity content of the core plasma and efficient power control in the divertor. In seeded type-III ELMy discharges a strong increase of the confinement with plasma pressure was observed. In parallel, a very moderate power flux in the outer divertor and a strong suppression of the W influx could be achieved. Investigations using a mixture N_2/Ar as seeding gas revealed a change in central particle transport compared to discharges with N_2 seeding only.

1. Introduction

Independent of the plasma facing materials (PFMs) in future fusion devices impurity seeding will become an inevitable element of operation to protect the divertor from excessive heat loads. Introducing low-Z to mid-Z impurities has also an impact on the erosion, especially that of a high-Z material, which is predominantly sputtered by the impact of impurity ions. The effective erosion flux will result from a delicate interplay between the increased flux of impurity ions and the reduction of sputtering yield due to the lowered divertor plasma temperature. At the same time the seed impurity concentration in the plasma core must be kept at a tolerable level. Optimisation of the divertor impurity enrichment and the radiation distribution between core, SOL and divertor might be required to resolve the issue for devices with high values of P/R (ratio of loss power and major radius). Another important constraint is the fact that the seeding scenario must be integrated into a small ELM regime or combined with ELM mitigation techniques.
While impurity seeding in present carbon devices is optional, it has become mandatory in the all-tungsten clad ASDEX Upgrade (AUG) [1] for high power conditions. Recent investigations on N_2 seeded plasmas yielded a very beneficial behaviour in terms of reduced power loads, moderate impurity concentrations and increased confinement [2]. Therefore, radiative cooling has been applied in a large variety of plasmas ranging from improved H-Modes at intermediate density and heating power [3] to discharges with very high heating power ($P_{aux} \approx 20$ MW) or high density and radiation fraction exploring the type-III ELM regime. The ultimate choice of the seeding gas is based on the temperature dependent radiation characteristics and operational considerations, namely the controllability of the plasma radiation and the influence on the confinement. Since the radiation efficiency of single gases suitable to be used in future

fusion devices varies considerably, gas mixtures could be used to achieve optimum radiative efficiencies $\Delta P_{rad}/\Delta Z_{eff}$ over a broad temperature range.
In Sec. 2 the radiation potential of different seeding gases for typical plasma edge conditions is presented and the feedback control scheme used in ASDEX Upgrade is sketched. In Sec. 3 the results for N_2 seeding in different discharge scenarios are described and Sec. 4 discusses the behaviour of W influxes and concentration with N_2 seeding. Finally, first experiments with the injection of gas mixtures are presented in Sec.5. Section 6 will conclude the paper.

2. Selection of seeding gas and control scheme

In a recent paper by Kallenbach et al. [4] the ingredients for radiative power removal, with the ultimate goal of achieving partial detachment of the outer divertor are reviewed. First, main plasma radiation is used to reduce the power flux over the separatrix. The radiative loss function L_z of a specific impurity can be calculated for core plasma conditions assuming coronal equilibrium and scales roughly with the atomic charge to Z^3. Therefore, heavier species are the more efficient seed species for core radiation, since they cause less fuel dilution. However, core radiative losses have to be limited to avoid negative effects on energy confinement and a too close approach of the H-L transition power threshold. In the trace limit, the core radiative losses scale linearly with the impurity concentrations. For the radiative power removal in the scrape-off layer (SOL) and the divertor low-Z species are best suited, which have a favourable radiative characteristics in the 10 eV temperature range. Since the impurity residence time in the divertor may be shorter than ionisation and recombination time scales, the radiative losses have to be calculated by a collisional radiative model (here, the ADAS database is used [5]) using time dependent ionisation equations, similar to the ansatz of a radiative potential introduced by [6]. In this framework a particle residence time τ is specified, which describes the timespan after which the evolution of the collisional-radiative processes in the divertor plasma is terminated [7]. Figure 1a) shows the corresponding radiative loss function for species of interest under divertor conditions for a product of density and residence time typical for AUG ($n_e\tau = 10^{16}$ m^{-3}s). Since under these conditions (recombination is not important) the ionisation time and the excitation time depend about linearly on the electron density (as long as multi-step processes are not important), the radiated power density per impurity atom depends only weakly on the electron density. These non-coronal conditions in the divertor plasma increase the radiative losses. For long residence times and higher emitting ionization stages, the radiative losses decrease towards their coronal values (see Fig.1b)). The final step towards acceptable peak power loads on a divertor target is the achievement of partial detachment, which relies on momentum losses leading to a pressure drop in front of the target. Since the most important momentum loss terms are recombination and charge exchange a relatively cold plasma is required to make these momentum loss mechanisms efficient [8]. This means that besides direct power dissipation, a major task of seed impurity radiation is to cool the plasma down to temperatures where momentum losses start to become efficient. Inspecting figure 1 reveals that for T_e below 10 eV, nitrogen and argon come

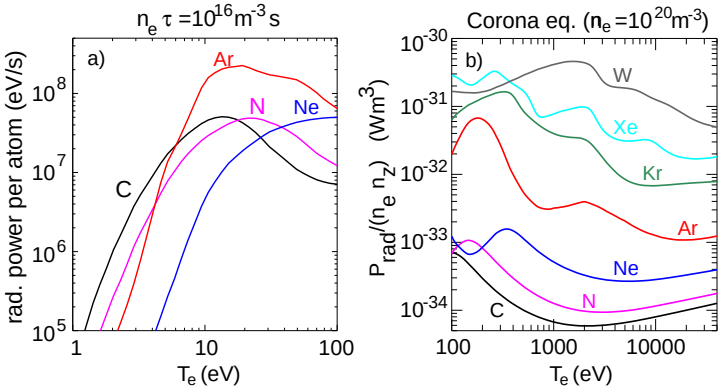

FIG. 1: Radiative potential (a), AUG divertor conditions) and radiation loss parameter (b), AUG core conditions) for different seed impurities (details see text).

closest to carbon, which is known as an efficient intrinsic coolant from experiments in devices with carbon PFCs. Neon exhibits comparatively low radiative losses at low electron temperatures. Argon has to be ruled out as strong divertor radiator in devices with moderate divertor impurity compression and low pumping speeds, since the required divertor concentrations in the per cent range are not compatible to the maximum allowed core concentration of a few per mille. In order to provide a flexible and optimized protection of the divertor from excessive heat loads, a feedback signal is required which is closely related to the target power load. There are several approaches, but their complexity is critical to a system relevant for machine safety. In ASDEX Upgrade, the ELM filtered (thermo-)electric current into a divertor tile, measured as voltage at a shunt resistor embedded in the tile mounting has been chosen as a feedback signal. This measurement probes mainly the temperature difference between the outer and inner divertor. The inner divertor has very low electron temperatures in between ELMs and therefore the thermoelectric current corresponds in good approximation to the outer divertor temperature as could be confirmed by Langmuir (LP) probe measurements. Since the interpretation of the measured signal in terms of a divertor temperature appeared more useful for operation and interpretation, the current is multiplied by a fixed factor obtained by comparison with LP data and is denoted T_e^{div} throughout this paper, with units of electron volts. Within this unit the error of the measurement is estimated to be smaller than 2 eV. For H-mode conditions, T_e^{div} was found to also represent a reasonable approximation of the outer divertor peak power load [9]. It turned out to be very simple and robust in real-time data acquisition and evaluation.

3. Results with nitrogen seeding

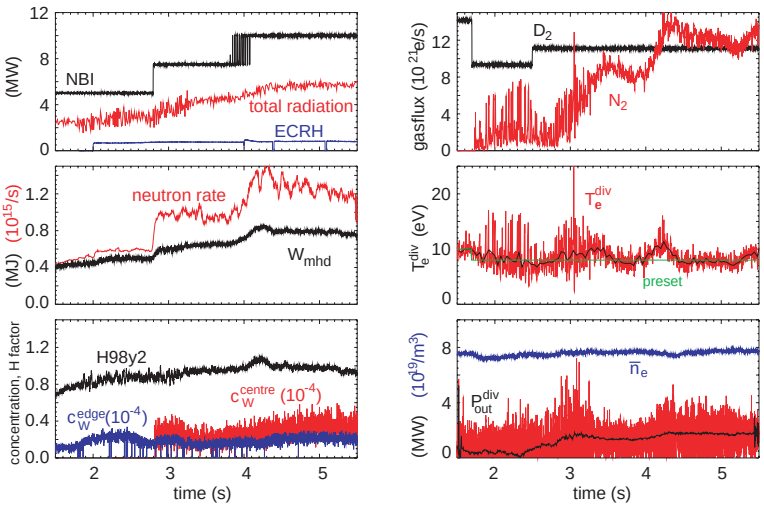

FIG. 2: N_2 seeded H-Mode discharge #25394 with $I_p = 1$ MA, $B_t = -2.5$ T. The D_2 puff was kept constant through the main phase of the plasma, whereas the divertor plasma temperature T_e^{div} was feedback controlled to 8 eV. Note the response of the N_2 puffing rate to the increase of heating power.

In first attempts performed with argon seeding a considerable fraction of central heating had to be used to avoid central impurity peaking. Moreover, since the radiative power removal by Ar takes place in the separatrix/pedestal region, the discharges were close to the H-L threshold causing large, low frequency type-I ELMs leading in turn to a strong increase of the bulk impurity level and radiation. Active ELM triggering by injection of small pellets was necessary to allow for steady operation [10]. In contrast using the same control scheme but N_2 instead of Ar as seeding gas, a very beneficial behaviour in terms of power load as well as impurity control could be achieved. However, wall storage of nitrogen in tungsten was found to have a significant influence on the necessary gas fluxes and on the nitrogen content of subsequent discharges making the feedback system indispensable [9]. Its qualitative behaviour, namely the N storage in the implantation range and the nitrogen release at elevated temperature, was found to be similar to that obtained in laboratory experiments [11]. Typical parameters of radiatively cooled discharges in AUG are $I_P = 1 - 1.2$ MA, which provides a current density and therefore a Greenwald density similar to ITER, and $B_t \approx -2.5$ T suitable for central heating with

2nd harmonic ECRH at 140 GHz, resulting in $q_{95} = 3.9 - 4.8$. The heating is varied from $P_{heat} \approx 6 - 20$ MW, representing at its upper end a P/R half that of ITER. The divertor temperatures are typically controlled to $T_e^{div} = 4 - 12$ eV resulting in D puffing rates $0.4 - 4 \cdot 10^{22}$ e s^{-1} and N_2 puffing rates $0.3 - 2.8 \cdot 10^{22}$ e s^{-1} (the rates are averaged over 200 ms and account for all electrons of the puffed particles). The D_2 was puffed in the outer midplane from 2-4 valves at toroidally different locations, whereas the N_2 was injected in the divertor below the X-point toroidally symmetric by 8 outlets. The achieved H-mode scaling factors $H98y,2$ were typically 0.9-1.1 in unseeded cases, depending mainly on the D puff level, and $H = 1.0 - 1.3$ in seeded cases [2–4]. Figure 2 shows a typical N_2 seeded discharge with T_e^{div} controlled to 8 eV. As can be seen in the inserts of the right column the power load to the outer divertor (P_{out}^{div}) is efficiently controlled by the feedback of T_e^{div}. Typically the line averaged Z_{eff} increases by 0.5 - 0.7 (1.5-2% N) in strongly N_2 puffed discharges. The Z_{eff} profile is found to be hollow, leading to central Z_{eff} clearly below 2 (see also Fig. 6). The radiation losses between and during type-I ELMs in ASDEX Upgrade with full tungsten walls have been compared for unseeded and nitrogen seeded discharges [12]. It has been found that the ELM averaged radiation level is about 60% of the input power in unseeded discharges (boronized full W AUG) and raises up to 80% in nitrogen seeded discharges. This increase is mainly caused by the increased radiation from the X-point and divertor region. There, the ELM averaged local radiation power is raised from 4-5 MWm^{-3} in unseeded discharges to more than 7 MWm^{-3} in nitrogen seeded discharges. Correspondingly the integrated radiated power from the X-point and the divertor increased by more than a factor of two from 5-10% of the input power to 15-20%. This increase is mainly caused by increased radiation between ELMs, the additional radiation during ELMs is nearly the same for both seeded and unseeded discharges. About 20-25% of the ELM energy is found as radiation in unseeded discharges and 30-40% with nitrogen seeding, due to the smaller ELM size (see Fig. 3). This value is comparable to the values found in former campaigns with mixed carbon and tungsten PFCs and in line with simulations at JET for ELMs with similar energy loss [13]. Consequently, the power load to the divertor targets during and in between type-I ELMs drops significantly with nitrogen seeding.

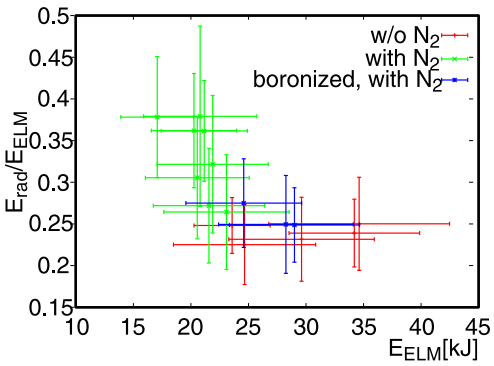

FIG. 3: Normalised ELM radiation E_{rad}/E_{ELM} versus ELM energy E_{ELM} in unseeded and N_2 seeded (unboronized/boronized) discharges.

In order to check the applicability of the radiation cooling to P/R levels as close as possible to the ITER target, discharges with 20MW heating power, including about 1 MW central ECRH in O2 mode were performed. Good energy confinement ($H98(y;2) = 1$) could be obtained simultaneously with a low impurity content of the core plasma ($Z_{eff} < 1.8$). Strong deuterium puffing has been used to enhance SOL/divertor radiation, and obviously the corresponding confinement degradation is compensated by the improvement caused by nitrogen. In these discharges, about half of the radiated power is emitted in SOL and divertor (see also [14]).

The performance and behaviour of type-III ELMy discharges was investigated in dedicated discharges at $I_P = 1.2$ MA with nitrogen seeding at high density ($n_e \approx 1.4 \cdot 10^{20}$ m^{-3}, $0.8 n_{Greenwald}$), high additional heating power ($P_{aux} \approx 14$ MW) and a high radiation fraction ($f_{rad} > 70\%$). The ELM type was identified by its dependence on power crossing the separatrix and its magnetic signature. The deposited power in the outer divertor was reduced to below 2 MWm^{-2} (average) and to an ELM peak power flux of only 3-4 MWm^{-2}. Moreover, the W influx was strongly

suppressed even during the ELMs (see Sec. 4). A rather low confinement ($H98(y,2) \approx 0.6$) was found at low β rising to $H98(y,2) \approx 1$ at $\beta_N \approx 2.3$, reflecting a similar improvement of the confinement with N_2 seeding as in the case of type-I ELMs.

4. Tungsten behaviour in nitrogen seeded discharges

The time resolved W influx is obtained spectroscopically by measuring the WI line radiation at 400.9 nm on 38 lines-of-sight covering the outboard divertor, some low field side limiters as well as the central column [15]. The measured photon flux density can be transformed into an eroded tungsten flux density using the inverse photon efficiency, i.e. the $S/XB \approx 20$ (at $T_e^{div} \approx 10$ eV) [16]. For lower divertor temperatures ($T_e^{div} < 5$ eV) the evaluation of the W flux gets more uncertain because of the strong temperature dependence of the related S/XB value [17]. One has to keep in mind that the spectroscopically derived W flux only yields an upper limit for the net influx / net erosion since under high density divertor conditions the eroded W atom gets quickly ionized and may be promptly redeposited within one gyro-orbit. Typical redeposition fractions in the divertor are $50-90\%$ [18,19].

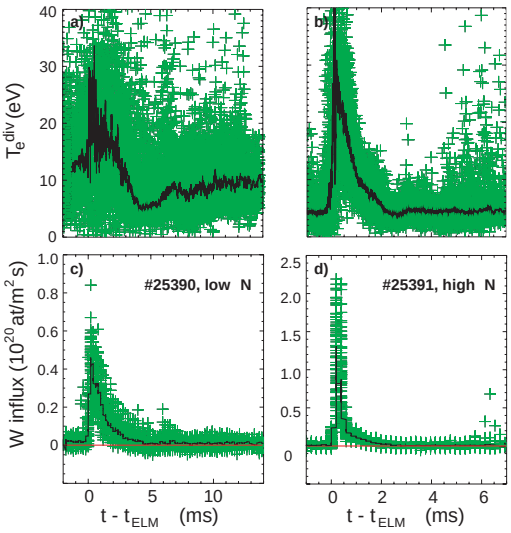

FIG. 4: Divertor temperature T_e (from Langmuir probe measurements) and W flux (from spectroscopy) after coherent averaging over many ELMs for 2 discharges with weak and strong nitrogen seeding.

Comparing a pair of unseeded and N_2-seeded discharges with the same heating power and the same level of D_2 puff, no difference in the time averaged W influx was found, neither in the main chamber at the low field side limiters nor in the divertor [9]. Since the radiation cooling by N is mostly provided in the divertor volume, little change in the main chamber SOL parameters is expected. However in the divertor the inter-ELM temperature decreased from about 12 eV in the unseeded discharges to the feedback controlled to $T_e^{div} = 7$ eV in the seeded discharge. Looking into more detail, the influence of N on the erosion during ELMs was investigated in a discharge series with about 11 MW auxiliary heating and a deuterium puff level of 0.8×10^{22} s^{-1}. The inter-ELM divertor temperatures were feedback controlled by nitrogen puffing to $T_e^{div} = 12$, 8 and 5 eV (#25390 – #25392), respectively. In discharge #25391 ($T_e^{div} = 8$ eV) the ELM frequency was about a factor 2 higher and the ELMs were a factor 3 shorter compared to #25390 ($T_e^{div} = 12$ eV). Concomitantly, the ELM energies were reduced from $W_{ELM} = 60$ kJ (#25390) to 20 kJ (#25391) whereas the requested N_2 puffing rate increased from $\Gamma_N \approx 0.3 \times 10^{22}$ e s^{-1} to $\Gamma_N \approx 1.4 \times 10^{22}$ e s^{-1}. Fig. 4 presents the coherent averaging of divertor electron temperature (from LP measurements) and of W influx measurements. Although the ELM energy is only one third of that with less N_2 cooling, the maximum W sputtering yield is 3 times larger during the ELM, leading only to a moderate reduction of the average W yield [4]. Obviously, the additional sputtering by N ions compensates for the lower T_e^{div}. Reducing the inter-ELM divertor temperature further to $T_e^{div} = 5$ eV (#25392) leads to an almost complete suppression of inter-ELM W-sputtering in line with TRIM calculations of the effective sputter yield using a few percent of N^{3+} impinging the W divertor targets [11].

In [20] the ELM averaged W influx is investigated for a large dataset of H-mode discharges at different input power and varying T_e^{div} or N_2 injection, respectively. As expected, the W influx in the divertor increases with increasing P_{aux} (energy and particle flux to the divertor). There

is, however, no clear trend for a reduction of the W influx with decreasing T_e^{div}. Only in discharges where in addition to the N_2 puff the D_2 puffing rate is increased to a very high level ($\Gamma_D = 4 \times 10^{22}$ e s^{-1}) the W influx is completely suppressed not only in between the ELMs, but also during the small ELMs (Type III ELMs) appearing at this high D_2 puffing level.

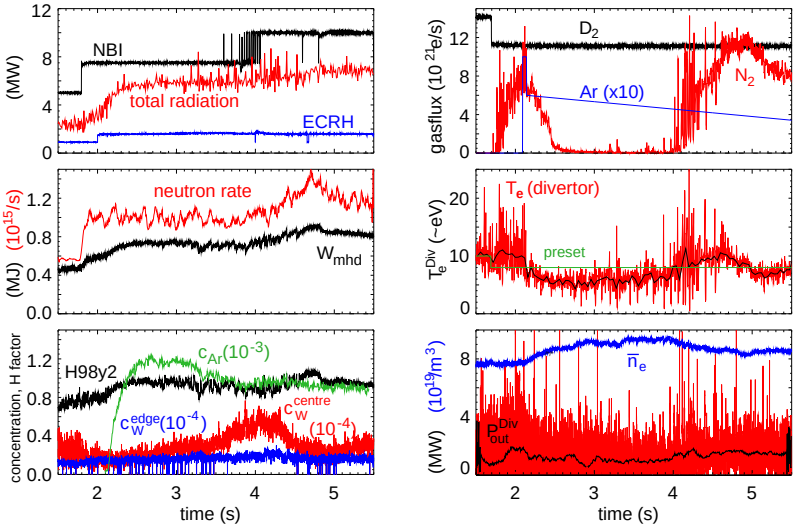

FIG. 5: Radiatively cooled discharge #25834 with simultaneous N_2 and Ar injection. The main plasma parameters are similar to that of Fig. 2 but with additional feed forward Ar seeding starting at 2.1 s. As a reaction to the Ar injection the N_2 puff is switched off by the feedback control. Note that the Ar puff rate is multiplied by 10 for better illustration.

The W concentration is deduced routinely in AUG from X-ray and VUV spectroscopy [21]. The use of spectral lines originating from charge stages around 30+ as well as around 46+ allows to distinguish peripheral ($T_e \approx 1.5$ keV) and central emissions $T_e \approx 3$ keV) for typical ASDEX Upgrade temperature profiles. Generally, there is no increase of the W concentration in N_2 seeded discharges compared to non seeded ones (see also [22]). This is exemplified in Fig. 2, where due to the feedback controlled divertor temperature the injection of nitrogen increases by a factor of more than 10 between t=2.8s and 3.5s and the W concentration remains constant. Moreover, there is no sign of W accumulation since c_W^{centre} is only slightly higher than c_W^{edge} throughout the whole discharge. This is true for all discharges with N_2 seeding provided there is central ECRH in the range of 10% of the total auxiliary heating power. The edge W concentrations are always in the range of (a few) 10^{-5} and the peaking is about two, although the N influx varies by a factor of 10. This observation is consistent with the earlier results that c_W^{edge} is dominated by the main chamber sources [15] - which barely change - provided that the W transport is invariant.

5. Experiments with injection of gas mixtures

For devices without strong pumping (AUG, JET, ITER), a mix of at least 2 seeding species should be used to optimize the spatial radiation distribution, with N_2 being the best option for the divertor. In JT60-U a mixture of Ne and Ar was used [23], allowing slightly higher confinement at high density/high radiation fraction. In AUG investigations were started using N_2/Ne or N_2/Ar simultaneously. While the divertor electron temperature was feedback controlled by the N_2 as described above, Ne or Ar were injected as a feed forward gas-puff. Fig. 5 shows a similar discharge to the one shown in Fig. 2, where only the heating phase with 7.5 MW from NBI is advanced by 1 s and $P_{ECRH} \approx 1.5$ MW instead of 0.8 MW. As soon as Ar is injected the feedback stops the N_2 injection because the divertor temperature is reduced sufficiently by the Ar radiation. After the further increase of the heating power the N_2 puff is switched on to control T_e^{div} again. The Ar puff is programmed in such a way that the central Ar concentration, which is provided by the absolutely calibrated measurement of X-ray radiation emitted from He-like Ar, stays about constant throughout the discharge, as can be seen from the lower left insert. Similar to the discharge with pure N_2 injection, the edge W concentration remains unchanged throughout the discharge. However, as soon as the Ar puff replaces the N_2 puff,

the central W concentration starts to rise leading to a maximum peaking of c_W^{centre}/c_W^{edge}=3. When the N_2 puff starts again the peaking decreases quickly again, albeit the Ar puff and the central Ar concentration remain almost unchanged. The strong influence of the Ar injection on the particle confinement is also reflected in the behaviour of the electron density, which immediately rises and starts to peak (not shown in the figure) although the number of injected electrons is much smaller during this phase (the increase of the Ar and W concentration cannot account alone for the increase of the electron density). In Fig. 6 the temporal behaviour of the Z_{eff}-profile is presented. Before the Ar injection, the profile is hollow. As soon as Ar is puffed and the N_2 injection decreases to zero, it strongly changes its shape: the edge Z_{eff} decrease and in the centre it increases slightly. Increasing the N_2 puff again (due to higher P_{aux}) the Z_{eff}-profile recovers its previous hollow shape. Part of this behaviour can be explained by the change in the ELM behaviour. Similar to the earlier experiments with Ar puffing [10] the ELMs are less frequent and larger in the Ar dominated phase ($f_{ELM} \approx 120$ Hz at 3.5 s, instead of 220 Hz in N_2 seeded reference case). An analysis of the particle transport using the behaviour of the spectral line of He-like Ar and soft X-ray profiles employing the gradient-flux method (similar to the procedure described in [24]) indeed shows a change in central particle transport parameters from the first phase at around 2.1-2.3 s, where N_2 is puffed in addition, to the phase around 2.5 - 3 s. During the later phase with Ar seeding only, the central diffusion coefficient for Ar is reduced by at least a factor of 3 down to approximately the neoclassical value.

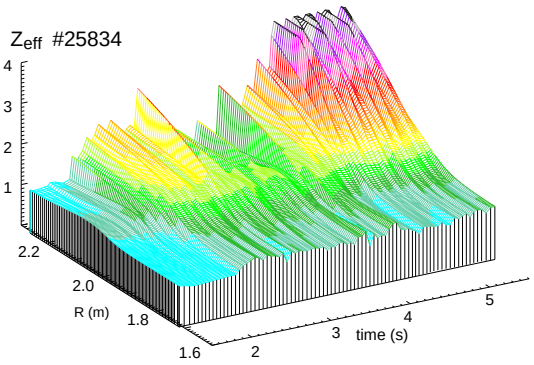

FIG. 6: Temporal evolution of the Z_{eff} profile in discharge #25834. In phases with dominant N_2 puffing the profile is hollow, whereas it flattens during the phase where the nitrogen puff is switched off during the Ar puffing.

6. Summary and conclusions

Impurity seeding has become necessary in the all-tungsten clad ASDEX Upgrade for high power conditions. A very beneficial behaviour in terms of reduced power loads, moderate impurity concentrations and increased confinement has been found in N_2 seeded discharges. Radiative cooling has been applied in a large variety of plasmas ranging from improved H-Modes at intermediate density and heating power to discharges with very high heating power ($P_{aux} \approx 20$ MW) or high density and radiation fraction exploring the type-III ELM regime. Generally, the radiated power from the X-point and divertor region increased in N_2 seeded discharges by more than a factor of two to about 20% of the total input power. There is also a slight increase of radiation from the edge of the main plasma, but the core radiation is almost unchanged. The radiation fraction during type-I ELMs is increased, mainly because the ELM size decreases with N_2 seeding. In unseeded discharges with a pure tungsten wall, about 20% of the ELM energy is radiated, which is clearly less than in earlier discharges with mixed carbon and tungsten PFCs. For nitrogen seeded discharges, however, the ELM energy is generally smaller, and about 40% of the ELM energy is radiated. This value is comparable to that found in former campaigns with mixed C/W PFCs and in line with simulations at JET for ELMs with similar energy loss. Consequently, the power load to the divertor targets during and in between type-I ELMs drops significantly with nitrogen seeding. In seeded type-III ELMy discharges with good confinement (H98(y,2) ≈ 1) at $\beta_N \approx 2.3$, power densities below 2 MWm^{-2} in the outer divertor and strongly suppressed W influx could be achieved. Although usually an improvement of energy confinement is observed using N_2 as seeding gas no increased W concentrations are observed, since

obviously the particle confinement is not improved. This is supported by the fact that there is no change of the line averaged density and no signatures of central density peaking. Moreover the sustained regular ELM activity prevents a strong inward transport of W across the pedestal region. Investigations using N_2/Ar as seeding gas revealed a reduction in ELM frequency and a change in central transport compared to discharges with N_2 seeding only. Experiments using gas mixtures have only started, but the deleterious effects accompanying pure Ar are strongly ameliorated, albeit not completely suppressed. An optimisation for different levels of heating power is envisaged to provide a broader data base for the extrapolation to ITER, where the use of at least two seeding gases with different radiation characteristics might be necessary to provide a sufficient radiative cooling.

References

[1] R. Neu,et al., Plasma Phys. Control. Fus. **49**(12B), B59–B70 (2007).
[2] O. Gruber, et al., Nucl. Fus. **49**(11), 115014 (2009).
[3] J. Schweinzer, et al., Confinement of Improved H-modes in the All-Tungsten ASDEX Upgrade, *this conference*, IAEA–CN–180/EXC/P2-07, 2010.
[4] A. Kallenbach,et al., Plasma surface interactions in impurity seeded plasmas, accepted for publ. in J. Nucl. Mater., (2010).
[5] H. P. Summers, The ADAS Users Manual (2006).
[6] U. Samm, et al., J. Nucl. Mater. **176-177**, 273 (1990).
[7] D. Post, et al., Phys. Plasmas **2**, 2328 – 2336 (1995).
[8] C. S. Pitcher, et al., Plasma Phys. Control. Fus. **39**(7), 1129–1144 (1997).
[9] A. Kallenbach, et al., Plasma Phys. Control. Fus. **52**(5), 055002 (2010).
[10] A. Kallenbach, et al., J. Nucl. Mater. **337-339**, 732–736 (2005).
[11] K. Schmid, et al., Nucl. Fus. **50**, 025006 (2010).
[12] J. Fuchs, et al., Radiation losses of type-I ELMs during impurity seeding experiments in the full tungsten ASDEX Upgrade, accepted for publ. in J. Nucl. Mater.(2010).
[13] J. Rapp, et al., Nucl. Fus. **44**(2), 312–319 (2004).
[14] A. Kallenbach et al., Overview of ASDEX Upgrade Results, *this conference*, IAEA–CN–180/OV3–1 (2010).
[15] R. Dux, et al., J. Nucl. Mater. **390-391**, 858–863 (2009).
[16] A. Thoma, et al., Plasma Phys. Control. Fus. **39**(9), 1487–1499 (1997).
[17] I. Beigmann, et al., Plasma Phys. Control. Fus. **49**, 1833–1847 (2007).
[18] D. Naujoks, et al., Nucl. Fus. **36**(6), 671–687 (1996).
[19] R. Dux, et al., Erosion and Confinement of Tungsten in ASDEX Upgrade, *this conference*, IAEA–CN–180/EXD/6–2 (2010).
[20] R. Neu, et al., Tungsten behaviour in radiatively cooled plasma discharges in ASDEX Upgrade, accepted for publ. in J. Nucl. Mater., (2010).
[21] T. Pütterich, et al., Plasma Phys. Control. Fus. **50**(8), 085016 (2008).
[22] A. Kallenbach, et al., Nucl. Fus. **49**(4), 045007 (2009).
[23] N. Asakura, et al., Nucl. Fus. **49**, 115010 (8pp) (2009).
[24] M. Sertoli, et al., Local effects of ECRH on argon transport in L-mode discharges at ASDEX Upgrade, subm. to Plasma Phys. Control. Fusion (2010).